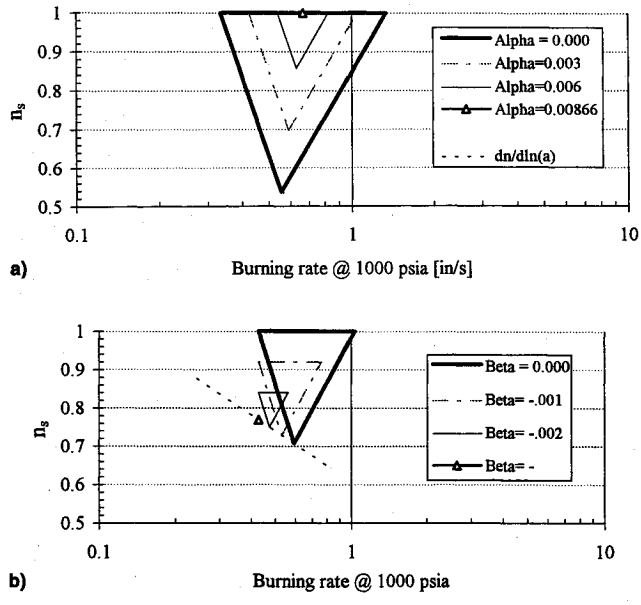

a)

b)

Fig. 2 Propellant ballistics diagram: a) $\alpha = 0.6-0.00866$, $\beta = 0.000$ and b) $\alpha = 0.00318$, $\beta = 0$ to -0.00289.

exponent propellant that satisfies the constraints. The maximum exponent N_{MAX} and standard exponent n_s are identical in this case.

As α' is increased, the triangular region becomes smaller. The minimum exponent increases until the burn rate curves span from line A–C to line B–D in Fig. 1, in which case

$$\alpha'_{MAX} = (N_{MAX} - A^1_n)/B^1_n, \qquad @(\beta = 0) \qquad (13)$$

giving the value of 0.00866 1/°F, which is plotted as the center point of Fig. 2a.

Effect of β at Constant α'

Figure 2b illustrates the effects of variations in the pressure exponent sensitivity for a fixed value of α'. In this case, α' is assumed constant at 0.00318 1/°F, while the exponent sensitivity ranges from 0 to −0.00289 1/°F. The variation in exponent sensitivity causes a reduction of the triangular solution space until it becomes a point at the maximum allowable value. The minimum exponent increases while its corresponding reference burning rate decreases.

Increasing the pressure exponent sensitivity then reduces and translates the propellant solution space to narrower exponent ranges and lower reference burning rates. The maximum value of pressure exponents also decreases as β increases [Eq. (12b)].

Conclusions

Propellant design relationships for variable exponent propellants have been developed and applied to a gas generator design problem. The method defines a region of acceptable propellant ballistic properties as a function of two propellant temperature sensitivity parameters. The design achieves mass flow rate, pressure, pressure exponent, and temperature range constraints. The propellant diagram approach gives the designer or propellant formulator a region of compliant ballistic properties for a given application instead of a single design point.

Acknowledgment

This work was sponsored by the Propulsion Research Center at the University of Alabama in Huntsville.

Effects of Kevlar® Fibers on Ammonium Perchlorate Propellant Combustion

M. H. Hites*
Illinois Institute of Technology, Chicago, Illinois 60616
and
M. Q. Brewster†
University of Illinois at Urbana–Champaign, Urbana, Illinois 61801

Introduction

MICROSCOPIC chopped Kevlar fibers were added to ammonium perchlorate (AP) composite propellants to investigate their burn rate enhancing features. Kevlar fibers have been used in the past[1] to increase the strength of AP composite propellants, but as a side effect it was observed that the fibers increased the burning rate of an AP/Al composite as much as 27% at 3.5 MPa. In the present work, steady burning rate measurements and combustion photography were used to quantify the burning rate enhancement and suggest a possible explanation for the observed increases.

Experimental

The steady burning rate was measured for the series of AP composite propellants shown in Table 1. The burning rate of each propellant was measured using the fuse wire technique in a nitrogen-purged combustion bomb. Strands of 7 × 7 mm cross section and 30–60 mm length were coated lightly with vacuum grease as an inhibitor and were ignited by nichrome wire. The initial temperature of strands was ambient room temperature (20–25°C).

High-speed and microscope photography were used to investigate the qualitative differences between the gas phase combustion and surface condition of the various propellants. Conventional VHS camcorder movies and 35-mm SLR macrolens photography were also used to reveal macroscopic differences between the propellants. Although only photographs from the 35-mm photography are presented here, some observations based on the other photographic techniques are discussed when applicable.

Results

Burning rate measurements of the nonmetallized propellants are shown in Fig. 1 along with the corresponding burning rate equation:

$$r = aP^n$$

where burning rate r is in mm/s and pressure P is in MPa. The coefficient a and exponent n were determined by a least-squares fit, and a linear correlation coefficient of 0.98 or better was calculated for each of the curve fits. Figure 1a shows that the addition of small amounts of Kevlar increased the burning rate and lowered the burning rate exponent slightly in nonmetallized AP systems. Figure 1b compares propellants with fiber lengths of 2 and 5 mm to a fiberless AP composite propellant and demonstrates increased burning rate with increased

Received Sept. 28, 1994; revision received April 26, 1995; accepted for publication Sept. 11, 1995.

*Research Assistant, Department of Mechanical and Aerospace Engineering, 10 West 32nd Street. Student Member AIAA.

†Professor, Department of Mechanical and Industrial Engineering, 1206 West Green Street. Associate Fellow AIAA.

Table 1 AP propellant formulations on a mass basis

Propellant	Oxidizer,[a] %	Binder,[b] %	Aluminum,[c] %	Fiber,[d] %	Carbon,[f] %
AP-1	79.0	20.0	—	—	1.0
AP-2	79.0	19.0	—	1.0	1.0
AP-3	61.25	20.0	17.75	—	1.0
AP-4	61.25	19.0	17.75	1.0	1.0
AP-5	80.0	20.0	—	—	0.1
AP-6	80.0	19.0	—	1.0[e]	0.1
AP-7	80.0	19.0	—	1.0	0.1

[a]Ammonium perchlorate 2/3 90 μm by mass.
[b]AP1–4 propellants: 84.0% HTPB, 6.0% isophorone diisocyanate (IPDI), 10.0% dioctyl aditate (DOA), one drop dibutyltin diacetate and AP5–7 propellants: 91.4% HTPB, 6.6% IPDI, 2% DOA, one drop dibutyltin diacetate.
[c]Nonspherical, nominal 15 μm.
[d]Kevlar Floc, 5 mm length.
[e]AP6 only: Kevlar Floc, 2 mm length.
[f]Cabot Regal 300R GP-3020 carbon black powder (used to increase opacity for pulsed-laser experiments not presented here).

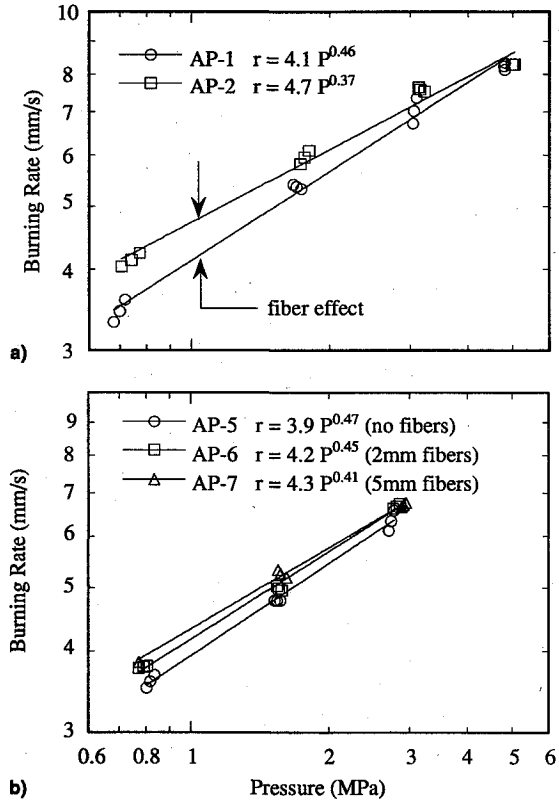

Fig. 1 a) Effect of fiber on nonmetallized AP propellants and b) effect of fiber length on nonmetallized AP propellants.

fiber length. In either case, the addition of 5-mm fibers resulted in about a 10% increase in burning rate at low pressure and a decrease of about 12–18% in pressure exponent over the baseline nonmetallized propellant.

Comparisons were also made between aluminum–metallized AP propellants with and without Kevlar fibers. It was observed (see Fig. 2) that adding 1% fibers increased the burning rate by approximately 25% at low pressure with a corresponding reduction in pressure exponent of about 25–30%. This was more than double the increase as compared to the nonmetallized propellants of Fig. 1. Figures 1 and 2 indicated that the addition of small amounts of Kevlar fibers increased the burning rate in both the metallized and nonmetallized propellants, but the effect was more predominant in the metallized propellant.

Several photographic methods were used to examine qualitative differences between metallized propellants with and without Kevlar fibers. Operating a VHS video camera at 1/1000 s shutter speed, it was seen that a distinct increase in surface

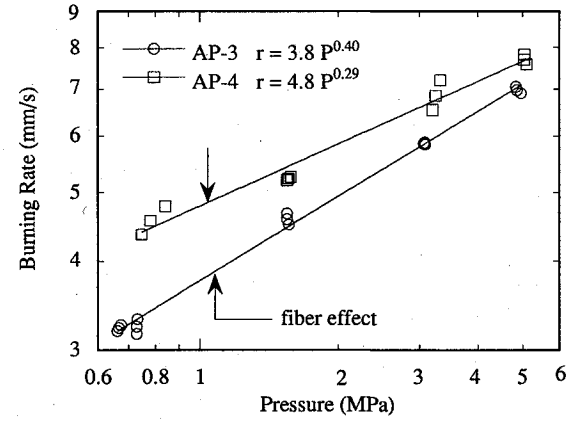

Fig. 2 Effect of fiber on aluminum–metallized AP propellants.

brightness occurred with addition of Kevlar. The camcorder did not produce significant resolution to determine the cause of the increased brightness, but it appeared that Kevlar fibers were protruding through the surface and glowing white just above the propellant surface, making them difficult to distinguish from the burning aluminum agglomerates.

Based on SLR camera photographs,[2] it appeared that the plume over the Kevlar propellant had greater smoke density than that of the nonfiber propellant, perhaps indicating a larger mass removal rate from the Kevlar propellant surface. It could be suggested the addition of the fiber resulted in a more fuel-rich propellant, producing the increased smoke density. However, in each of the Kevlar propellants, the fibers directly replaced the hydroxyl terminated polybutadiene (HTPB) binder so that the fuel-to-oxidizer ratio was maintained as constant as possible between the different formulations.

Another feature observed with the Kevlar propellant was luminous streaking of the combustion gases just above the surface of the propellant. These streaks were believed to be an effect of Kevlar fibers protruding into the gas phase and locally anchoring flames closer to the surface. Although some streaking is seen off the surface of most composite propellants, the photographs of the Kevlar metallized propellant apparently demonstrated the presence of obstructions larger than the normal filigrees on the surface of burning propellants.

Figure 3 shows two microscope photographs taken during the burning of propellant AP-4 at atmospheric pressure. These photographs show that the Kevlar fibers protruded through the surface, both in single strands and in small clumps of loosely packed fibers. Figure 3b shows an irregular burning surface that may have resulted from a localized increase in burning rate due to the fibers. Furthermore, additional microscope and high-speed photographs of burning AP propellant (not presented here) revealed what appeared to be smaller aluminum

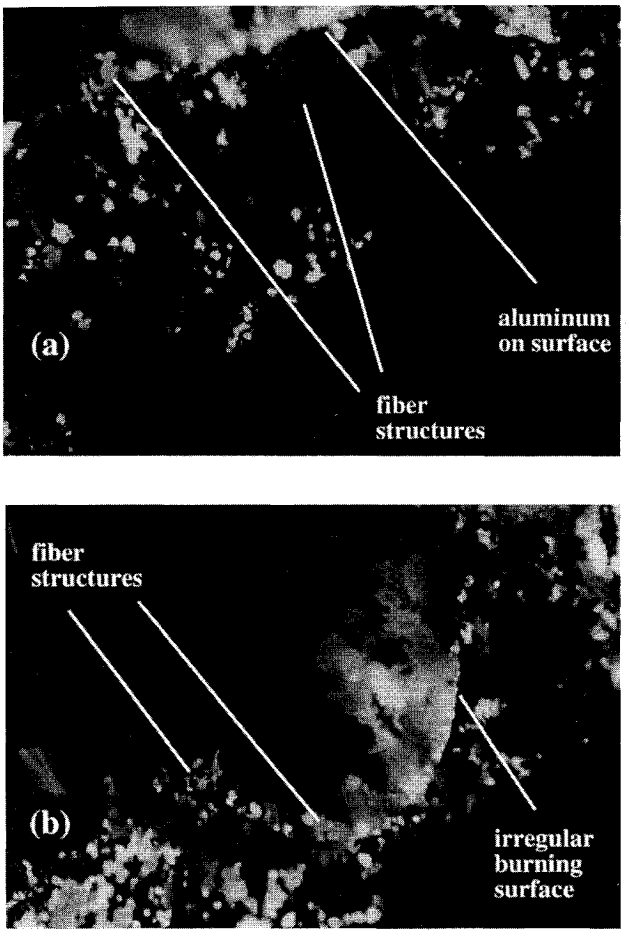

Fig. 3 Microscope photographs of burning aluminium–metallized propellant with fibers at atmospheric pressure: a) typical and b) irregular burning surfaces.

agglomerates on the surface of the fiber propellants as compared to larger agglomerates on the surface of the fiberless metallized propellant.

Discussion

In each set of propellants, it was observed that the burning rate exponent decreased with the addition of Kevlar fibers, and also that the most substantial burning rate enhancement due to the fibers was seen at lower pressures. An explanation can be suggested for both of these observations. At low pressure (≈1 MPa), the primary flame standoff distance apparently was great enough that the protruding Kevlar fibers could improve substantially the burning rate by anchoring the flame closer to the propellant surface. As pressure increased (above 1 MPa) the primary flame was pushed closer to the surface, and since Kevlar fibers appeared to protrude through the surface, the result of the flame moving closer would be earlier destruction of the Kevlar fibers. Eventually, the flame would be so near the surface that the Kevlar fibers would not protrude at all and have no effect on the burn rate. Moreover, comparing the curves in Figs. 1 and 2, it appears that the burning rate curves will intersect and cross at some high pressure because of the change in pressure exponent in the Kevlar propellants. However, based on the previous discussion, at higher pressure the flame should be close enough to the surface that the protruding fibers would be burned immediately and would not affect the gas phase combustion. Consequently, the two burning rate curves should converge at high pressure, not intersect.

With the aid of photography and steady burning rate measurements, a mechanism for burning rate enhancement due to the addition of Kevlar fibers can be hypothesized. Several mechanisms were considered as explanations for the burning rate enhancement due to the addition of Kevlar fibers: 1) protruding fibers acting as light pipes channeling radiant energy below the surface, 2) fibers anchoring the flame closer to the surface and igniting decomposition products closer to the surface, and 3) protruding fibers retaining metal and oxidizer particles near the surface for longer periods of time. In each of these cases, the net result would be an increase in surface (or subsurface) heat transfer, implying an increase in burning rate.

Of these ideas, flame anchoring or glow plug ignition seem to be the most likely mechanism. As reported by Dold[3] and Lewis,[4] for high blowing velocity (or high burn rate), the flame can be anchored with a wire protruding into the flame. In the case of a composite propellant, if a wire or fiber were extended through the surface and into the gas phase, flame anchoring could occur, improving the stability of the flame and limiting flame blowoff. This would produce an increase in conductive, and perhaps radiative, heat feedback to the surface of the burning propellant.

With the Kevlar fibers protruding so far into the gas phase, it could be argued that the fibers were actually retaining the burning aluminum close to the surface for longer periods of time. This seems unlikely based upon the examination of the microscope photographs of the metallized propellant with fibers. It was observed that the fibers protruded through the surface, but not at a density that would have prohibited the movement of the aluminum particles. Additionally, if an aluminum agglomerate were to ignite near a Kevlar fiber, the heat transfer from the burning droplet would probably destroy the fiber since the decomposition temperature of the fibers is on the order of 1000 K. These observations make aluminum retention a less likely explanation than the flameholder idea.

It was observed that the aluminum agglomerates on the surface of the faster-burning Kevlar propellant AP-4 appeared smaller than those of the non-Kevlar propellant AP-3. This is consistent with Brewster and Hardt[5] and Price[6] who have shown that smaller flame standoff distances (and thus higher burning rates) are generally associated with lower aluminum agglomeration and smaller agglomerates. In the present study, if the fibers in AP-4 were anchoring the flame closer to the surface locally, then the flame standoff distance would decrease locally, resulting in smaller agglomerates and an overall increase in burning rate. This may help explain the larger burning rate increase seen with the metallized propellants in Fig. 2 as compared to the nonmetallized propellants in Fig. 1.

Summary

The steady burning rate of AP composite propellants with and without Kevlar fibers was investigated using the fuse wire technique. Measurements over the pressure range 0.6–5 MPa revealed that the burning rate increased with the addition of 1% chopped Kevlar fibers. It was observed that the burning rate increased about 25–30% for metallized propellant at 1.0 MPa and less than 10% for nonmetallized propellant at 1.0 MPa due to the fiber additive. High speed and microscope photography suggested evidence that the burning rate enhancement may be due to a flameholding effect of unburned Kevlar fibers protruding through the propellant surface and into the gas phase. It was postulated that the modest increase in burning rate for nonmetallized propellant was due to the flameholder mechanism, while the metallized propellant burning rate increase may have included a combination of both the flameholder and small agglomerate effect. These results also have some interesting implications for the possibility of stabilizing solid rocket motors by reducing the dynamic burning rate pressure sensitivity using fiber additives.

Acknowledgment

The financial support of Thiokol Corp. for this research, and the NASA Space Grant for manuscript preparation, is greatly appreciated.

References

[1]Young, M., personal communication, Beltran, Inc., Brooklyn, NY, 1990.

[2]Hites, M. H., "Combustion of Metalized Propellants with Kevlar Fibers," M.S. Thesis, Univ. of Illinois at Urbana–Champaign, IL, 1992.

[3]Dold, J. W., "Flame Propagation in a Nonuniform Mixture: The Structure of Anchored Triple-Flames," *Dynamics of Reactive Systems*, Vol. 113, Progress in Astronautics and Aeronautics, AIAA, Washington, DC, 1988, pp. 240–248.

[4]Lewis, B., *Combustion, Flames, and Explosions of Gases*, 3rd ed., Academic, London, 1987, pp. 233–236.

[5]Brewster, M. Q., and Hardt, B. E., "Influence of Metal Agglomeration and Heat Feedback on Composite Propellant Burning Rate," *Journal of Propulsion and Power*, Vol. 7, No. 6, 1991, pp. 1076–1078.

[6]Price, E. W., "Combustion of Metalized Propellants," *Fundamentals of Solid-Propellant Combustion*, Vol. 90, Progress in Astronautics and Aeronautics, AIAA, New York, 1984, pp. 479–513.

Hot-Streak Clocking Effects in a 1-1/2 Stage Turbine

Daniel J. Dorney*
Western Michigan University, Kalamazoo, Michigan 49008-5065
and
Karen Gundy-Burlet†
NASA Ames Research Center, Moffett Field, California 94035

Nomenclature

C_t = ratio of local-to-freestream temperature
X = axial distance

Introduction

GAS turbine combustors can contain both circumferential and radial temperature gradients. These temperature gradients arise from the combination of the combustor core flow with the combustor bypass and combustor surface cooling flows. It has been shown both experimentally (e.g., Ref. 1) and numerically (e.g., Ref. 2) that temperature gradients can have a significant impact on the secondary flow and wall temperature of the first-stage rotor. A recent numerical study has shown that this phenomenon can also extend to second-stage stator airfoils.[3] A combustor hot streak such as this has a greater streamwise velocity than the surrounding fluid, and therefore, a larger positive incidence angle to the rotor (or other downstream blade row) as compared to the freestream. For hot streaks that do not impinge upon the first-stage stator airfoils, the rotor incidence variation through the hot streak and the slow convection speeds on the pressure side of airfoil surfaces combine to cause the hot-streak gases to accumulate on the pressure surfaces of downstream blade rows. The focus of the current effort has been to study the effects of the combustor hot-streak position on the temperature distributions of downstream airfoil surfaces. Two- and three-dimensional unsteady Navier–Stokes analyses have been used to study a 1-stator/1-rotor/1-stator/1-hot-streak configuration, and determine the impact of the combustor hot-streak position on the time-averaged first-stage rotor and second-stage stator surface temperatures.

Received April 29, 1995; revision received Nov. 13, 1995; accepted for publication Dec. 20, 1995.

*Assistant Professor, Department of Mechanical and Aeronautical Engineering. Senior Member AIAA.

†Research Scientist, Design Cycles Technology Branch. Senior Member AIAA.

Solution Procedure

The two- and three-dimensional computational analyses use a time-marching, implicit, finite difference scheme. The procedure is third-order spatially accurate and second-order temporally accurate. The inviscid fluxes are discretized according to an upwind-biased scheme, whereas the viscous fluxes are calculated using central differences. An alternating direction, approximate-factorization technique is used to compute the time-rate changes in the primary variables. In addition, Newton subiterations are used at each global time step to increase stability and reduce linearization errors. In this study, two Newton subiterations were performed at each time step.

Numerical Experiments

A series of numerical simulations of hot-streak migration through a 1-1/2 stage turbine have been conducted using both two- and three-dimensional unsteady Navier–Stokes procedures. The geometry used in the experimental hot-streak tests was the 1-1/2 stage turbine configuration of the United Technologies Large Scale Rotating Rig (LSRR) (Ref. 1). For the hot-streak experiments, the LSRR was configured to resemble the first 1-1/2 stages of a high-pressure turbine, typical of those used in aircraft gas turbine designs. In the experiment[1] and previous numerical studies,[2] the hot streaks were introduced between two stator airfoils of the LSRR. The temperature of the hot streak was twice that of the surrounding inlet flow, whereas the hot-streak static and stagnation pressures were identical to the freestream. The hot streak was seeded with CO_2 and the path of the hot streak determined by measuring CO_2 concentrations at various locations within the turbine stage using the blade surface static pressure taps. In the current two-dimensional numerical simulations, the hot streak is introduced to the inlet of the first stator passage in the form of a sine-wave temperature profile. In the three-dimensional simulations, similar to the experiment, the hot streak is modeled as a circular jet at 40% of the span. In both the two- and three-dimensional simulations, the hot-streak position has been varied in the gapwise direction along the first-stator inlet. The two positions of primary interest are 1) when the hot streak does not impinge on the first-stage stator and 2) when the hot streak fully impinges upon the first-stage stator. A hot-streak temperature of 1.2 times that of the surrounding inlet flow was chosen for this investigation.

The computational grid topology used in the 1-stator/1-rotor/1-stator/1-hot-streak two-dimensional simulations contained 29,733 computational grid points. The two-dimensional simulations were run for 18 blade-passing cycles, at 3000 time steps per cycle, on a DEC Alpha 3000-400 workstation. The computational grid used in the three-dimensional simulations contained approximately 2,700,000 grid points. The three-dimensional simulations were run for 10 cycles on a Cray C90 supercomputer.

Two-Dimensional Simulations

Figure 1 shows the minimum, maximum, and time-averaged surface temperatures along the surface of the rotor for the case in which the hot streak does not impinge upon the first stator. The temperatures along the suction surface show large excursions from the time-averaged temperature distribution, while the variations along the pressure surface are much smaller. The time-averaged temperatures along the pressure surface of the blade, however, are higher than along the suction surface. This phenomenon is similar to that observed in previous experiments[1] and numerical simulations,[2] in which the hot streak was